Laser-Plasma Interactions in a Single Hot Spot

D. S. Montgomery, J. A. Cobble, J. C. Fernández, and R. P. Johnson (P-24); H. A. Rose (T-13); R. Focia (Massachusetts Institute of Technology); and N. LeGalloudec (University of Nevada, Reno)

Introduction

Understanding the growth and saturation of laser-driven parametric instabilities such as stimulated Raman scattering (SRS—the scattering of light as it passes through a plasma; the light undergoes a change in frequency due to a change in the vibrational frequency of the scattering plasma waves), stimulated Brillouin scattering (SBS—light scattering by sound waves in the plasma), and self-focusing is important for the success of laser fusion. These instabilities can occur throughout the underdense (transparent) plasma in targets designed to achieve ignition, such as those for the proposed National Ignition Facility (NIF)[1], and may also constrain experimental designs for weapons physics and high-energy-density physics experiments planned on NIF. One major reason researchers are concerned with laser-plasma instabilities (LPI) is that they can significantly reduce the amount of laser energy absorbed by the target. Other deleterious effects can be produced by these instabilities such as target preheat due to fast electrons generated by SRS and degradation of the implosion symmetry caused by flow-induced beam steering, beam spraying, and crossed-beam energy transfer. Quantitative prediction of the onset and saturation of these instabilities under given laser and plasma conditions is the goal of research in this field, and will lead ultimately to their control.

Both SBS and SRS are three-wave processes which involve the resonant decay of the incident laser wave into a scattered light wave and a plasma wave. The instabilities must satisfy the frequency and wave-vector matching conditions

$$\omega_0 = \omega_s + \omega_{es}$$
$$\vec{k}_0 = \vec{k}_s + \vec{k}_{es} \qquad (1)$$

where ω, $\vec{k}$ are the frequency and the vector wavenumber of the waves, and the subscripts *0*, *s*, and *es* refer to the incident, scattered, and electrostatic plasma waves. For SBS, the plasma wave is a low-frequency ion acoustic wave (IAW), whose dispersion is approximately $\omega_{es} \cong c_s k_{es} + \vec{v} \cdot \vec{k}_{es}$, where c_s is the sound speed and v is the local flow velocity. The plasma wave involved in the SRS process is a high-frequency electron-plasma wave (EPW), with a frequency given approximately by the Bohm-Gross dispersion

$$\omega_{es}^2 \cong \omega_p^2 + 3k_{es}^2 v_{th}^2,$$

where $\omega_p = \sqrt{4\pi n_e e^2 / m_e}$ is the electron plasma frequency which depends on the electron plasma density n_e, and v_{th} is the electron thermal speed.

A major complication in understanding these instabilities is that the plasma waves created by these processes can interact with other waves in the plasma, can interact with each other, and can interact with the particles or bulk plasma to modify the background laser and plasma conditions. However, much progress has occurred in recent years in qualitative understanding of the onset, saturation, and interplay between these instabilities. This may be attributed in part to the use of beam-smoothing techniques such as random phase plates (RPP), which smooth the large-scale spatial structure often found in high-power lasers. The focal-plane intensity distribution created

in vacuum by a RPP consists of an ensemble of fine-scale hot spots or speckles with well-defined statistical properties. An example of a RPP-smoothed laser beam is shown in Figure 1a. The characteristic size of each speckle (hot spot) is related to the diffraction limit of the focusing optic (*i.e.* the width and length are $d_{sp} \sim f \lambda_0$ and $\mathcal{L}_{sp} \sim 7 f^2 \lambda_0$ respectively, where f is the ratio of focal length to beam diameter, and λ_0 is the laser wavelength). Recent work has demonstrated the importance of the laser hot-spot distribution in determining the onset behavior for SBS and SRS.[2,3]

Experimental History

In the absence of a quantitative predictive capability for laser-plasma instabilities, experiments have traditionally been performed in the largest possible laser-plasma volume using the largest available lasers in order to attempt to extrapolate the results to the even larger plasma volumes expected for NIF experiments. The plasmas produced in these scaling experiments are often quite complex and dynamic,[4,5] and may not mimic all aspects of NIF plasmas. Additionally, the instabilities can be *interdependent* in a laser beam with an ensemble of hot spots, and issues such as seeding and coupling of instabilities between hot spots arise and complicate our understanding of these processes. Further, because there is a distribution of laser intensities, SRS, SBS, or self-focusing can all occur to some extent throughout the laser-plasma volume, depending on the local intensities. All of these factors contribute to our lack of confidence in extrapolating the results of these scaling experiments to NIF. We must take a more fundamental approach to laser-plasma instabilities in order to develop a quantitative predictive capability for large plasmas.

The laser-plasma volume for ignition-scale plasmas is too large to be modeled from first principles using either current or planned advanced computing resources due to the relatively small spatial and time scales over which the instabilities occur. The smallest fundamental volume where the instabilities occur in a realistic laser beam is within a single laser hot-spot volume. The intensity pattern from an idealized single hot spot is well defined compared to the wide range of intensities present in the ensemble of hot spots in a realistic laser beam. Present computational resources are capable of performing first-principles calculations of LPI at the single-hot-spot volume. Therefore, experimental and computational studies of the coupling and saturation of instabilities in a single laser hot spot is a key first step to quantitative understanding of these processes in realistic ignition-scale laser plasmas.

This approach utilizes the detailed measurements from single-hot-spot LPI experiments to develop and benchmark *ab initio* models. The models would then be used to reduce the detailed microscopic processes to a simpler physical model (reduced or mesoscale model). Because most processes arising from the instabilities are localized within the hot-spot volume, the reduced model would serve as a sort of equation-of-state for the instabilities, averaging over the detailed microscopic processes. The reduced models could then be incorporated into the large hydrodynamic codes used to design NIF targets, and benchmarked against experiments with large laser-plasma volumes.

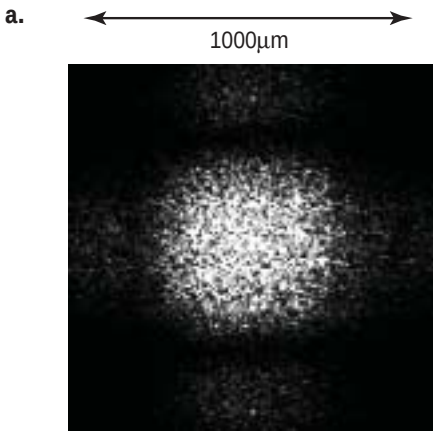

Figure 1a.Plot of the intensity pattern at best focus for a laser smoothed by using a random phase plate (RPP). The focal pattern is typical for large-scale laser experiments and those planned for NIF. The intensity pattern consists of thousands of individual hot spots or speckles.

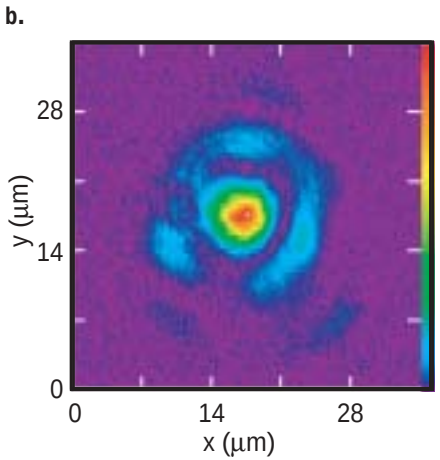

Figure1b. Plot of the measured intensity pattern at best focus for the single-hot-spot laser used in these experiments. Its size is similar to one of the hot spots found in the ensemble of hot spots in a RPP beam.

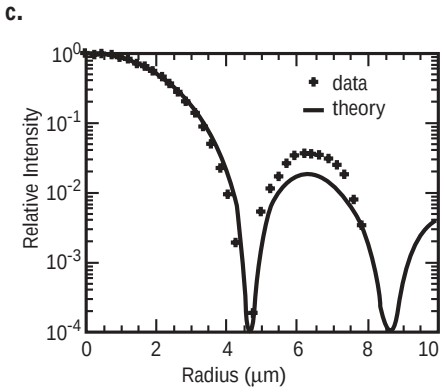

Figure1c. Plot of the measured intensity profile at focus for the single-hot-spot laser, compared to the theoretical curve for an ideal laser beam. The laser-beam intensity pattern is very similar to that of an ideal beam.

Laser and Plasma Conditions

The laser and plasma conditions for single-hot-spot experiments must be well characterized in order to compare the data directly to numerical models. The experiments were performed at the TRIDENT laser facility.[6] One of the three 527-nm laser beams was used to create and heat a 1-mm size plasma, which is large compared to a single-hot-spot volume. The single-hot-spot (diffraction limited) laser was produced by configuring a second, lower-energy laser to generate minimal wavefront distortion so that a nearly ideal diffraction-limited beam is produced. Lateral shearing interferometry was used to measure the relative wavefront quality of the 527-nm beam. Fringe analysis shows that the root-mean-square wavefront distortion is ~0.3 λ_0 over 90% of the aperture, and the wavefront is fairly reproducible for each experiment.

The single-hot-spot laser is focused using a high-quality lens with a beam diameter to focal length ratio of either f/4.5 or f/7. The focal plane intensity distribution of the single hot spot was measured *in situ* using a high-quality 40× microscope objective and a charge-coupled device (CCD) camera. Figure 1b shows an image of the interaction laser at best focus, and an azimuthally averaged radial profile is also shown in Figure 1c. The data show a nearly classic Airy pattern for a circular aperture. Superposed is the theoretical radial profile for diffraction from a plane wave incident on a circular aperture at f/7, and is in excellent agreement with the measured results. The focal spot deviates somewhat from the perfect diffraction limit in that there is more energy beyond the first Airy minima.

The interaction laser has a full width at half maximum (FWHM) of 3.8 ± 0.15 μm for f/7 focusing, and produces a peak intensity of 1.0×10^{16} W/cm^2 for a nominal energy of 0.8 J (max), in a 200-ps FWHM Gaussian pulse. The peak intensity is ~1/2 the peak intensity for a perfect diffraction-limited focus. The laser power output is kept roughly constant to maintain beam quality, and the peak intensity can be adjusted over the relevant range of intensities (10^{14}–10^{16} W/cm^2) using polished, calibrated neutral density filters.

The plasma was characterized using collective Thomson scattering from the heater beam by measuring spatial profiles of thermal levels of EPWs or IAWs using gated-imaging spectroscopy. The instrument collects the Thomson scattered light and spatially resolves the spectrum along the direction of plasma expansion. Profiles of the electron temperature (T_e), ion temperature (T_i), and flow velocity (v_z) along the direction of plasma expansion are obtained from measurements of the Thomson IAW spectra. The electron-density (n_e) spatial profile is obtained from measurements of the Thomson EPW spectra. A sample IAW spectrum is shown in Figure 2, and the measured plasma profiles are plotted in Figure 3 for a typical experiment. These measurements, together with the laser measurements, provide the initial conditions for comparing our data with the theoretical models.

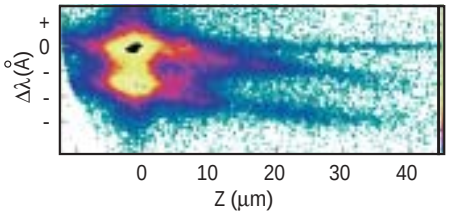

Figure 2. Time-resolved snapshot of imaging Thomson scattering spectra from thermal levels of ion acoustic waves. The waves are resolved as a function of distance from the target surface. The separation between the two peaks provides a measure of the electron temperature, and the spectral shift provides a measure of the flow velocity. Details of the spectral shape provide a measure of the ion temperature.

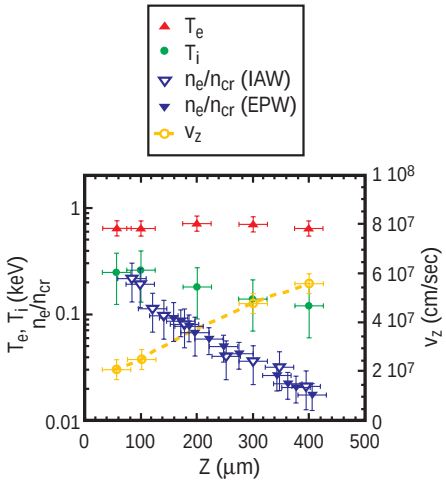

Figure3. Typical measured profiles of the electron temperature, ion temperature, electron density, and flow velocity plotted versus distance from target. These data are all obtained from the imaging Thomson scattering spectra.

Flow-Induced Beam Steering

Supersonic plasma flow past a laser beam resonantly drives ion acoustic waves and scatters the laser power in the flow direction; this results in deflection of the laser beam. This instability is a branch of the forward SBS instability and can deflect the laser by several degrees. This is an important effect for inertial-confinement fusion (ICF) target designs because near-sonic transverse flows can exist in regions of high laser intensity and may affect capsule implosion symmetry.

Measurements of the laser beam angular distribution are made after it has propagated through the plasma. Figures 4a and 4b show plots of the transmitted-beam angular distribution at two different intensities for a plasma with Mach ≈ 2 supersonic flow. The beam is deflected in the downstream flow direction and shows an interesting bow-like structure. Other instabilities such as SRS and SBS were negligible for these experiments at sufficiently low laser intensities. Therefore, the beam-deflection results can be directly compared to models that contain only the beam-steering and self-focusing physics over this range of intensities.

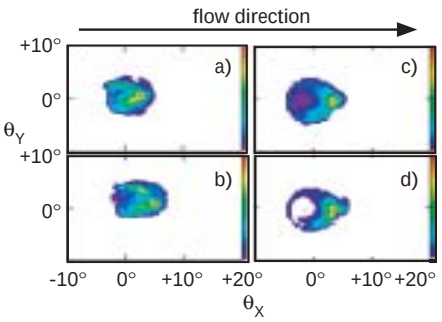

Figure 4. Transmitted beam angular distribution showing the effects of flow-induced beam steering from experiments with laser intensity of (a) 1.1×10^{15} W/cm² and (b) 2.7×10^{15} W/cm². Note the bow-like curvature toward the direction of flow. Three-dimensional (3-D) direct numerical simulations of these experiments are shown for a laser intensity of (c) 7.5×10^{14} W/cm² and (d) 1.5×10^{15} W/cm².

The experiment was compared to a three-dimensional (3-D) hydrodynamic model that solves a wave equation for the forward propagating light waves but neglects SRS and SBS backscattering. Figures 4c and 4d show plots of the transmitted-beam angular distribution from the 3-D model, using the initial conditions obtained in the experiment, and are remarkably similar to the experimental results. In order to be more quantitative, profiles taken parallel and perpendicular to the flow direction from the measurements and simulation results are shown in Figures 5a and 5b. The comparison is quite good in the parallel direction, but the simulation underestimates the amount of scattering in the perpendicular direction. Figure 6 shows a plot of the deflection angle in the flow direction from the experiment and model for a range of laser intensities. This represents the first successful quantitative comparison between a direct numerical simulation and a LPI experiment.[7] The good quantitative agreement is encouraging for the soundness in developing quantitative modeling using the single-hot-spot approach.

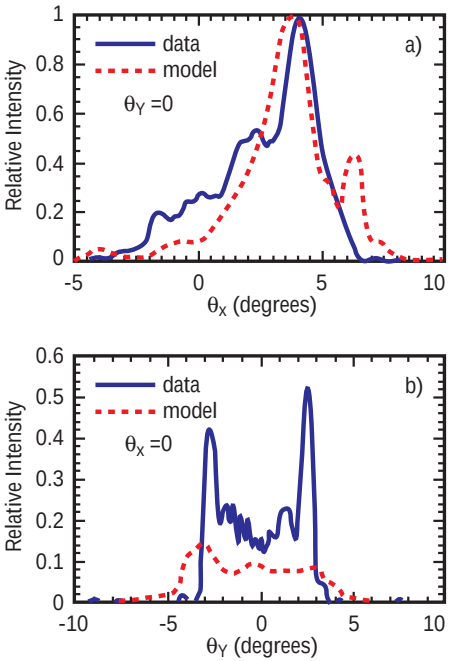

Figure5. Comparison of transmitted beam angular distribution (see Figure4b) for an experiment with peak laser intensity of 2.7×10^{15} W/cm^2. Three-dimensional direct numerical simulations were performed for these experimental conditions. Profiles of the measured and simulated transmitted beam distribution are shown (a)parallel to the flow direction and (b)perpendicular to the flow direction. Quantitative comparison between the measured and simulated profiles allow us to benchmark and refine our modeling.

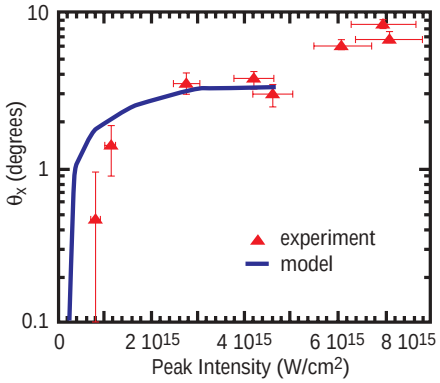

Figure6. Plot of deflected beam centroid versus peak laser intensity for the experiments (triangles) and the 3-D model (solid line). The experimental results are in good agreement with the 3-D modeling and represent the first-ever quantitative comparison between a laser-plasma instability experiment and modeling.

Stimulated Raman Scattering Growth

We studied SRS backscatter in these plasmas at low enough densities such that the electron plasma wave involved in SRS growth should be strongly damped according to classical theory. Figure 7 shows a typical plot of the time-resolved SRS spectra from a low-density experiment. According to Equation 1 (see page 82), the laser wave frequency is the sum of the scattered light frequency and the EPW frequency for the SRS process. Therefore, the EPW frequency, which depends on the electron density, is easily calculated from the scattered light spectrum. The relatively narrow SRS spectrum is indicative of the expected density uniformity over the hot-spot volume. Figure 8 shows a plot of the SRS reflectivity as a function of laser intensity. SRS grows rapidly up to intensities $\sim 2 \times 10^{15}$ W/cm^2, at which point the SRS reflectivity saturates and grows very little with laser intensity.

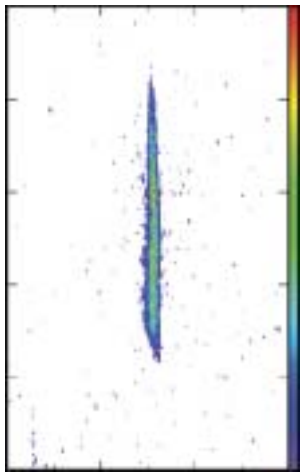

Figure7. Time-resolved SRS spectrum from a typical single-hot-spot experiment in the so-called "strongly damped" regime. The SRS typically lasts for the duration of the laser pulse (~200 ps). The narrow spectral width (~2nm) indicates that the SRS instability occurs in a plasma with a fairly uniform density.

We can estimate the expected SRS reflectivity with a simple comparison to classical analytic theory. The theoretical SRS reflectivity depends exponentially on a gain factor, $R_{SRS} \sim e^G$, where the gain factor $G \propto I \cdot L_{sp} / \nu_{EPW}$, I is the single-hot-spot peak intensity, L_{sp} is the single-hot-spot speckle length, and ν_{EPW} is the electron plasma wave damping that depends on the electron density and temperature. Assuming a static value for L_{sp}, and calculating ν_{EPW} based on the measured plasma conditions, one can easily estimate the SRS reflectivity versus intensity from classical linear theory. The classical theory estimate of SRS reflectivity is also shown in Figure 7 and predicts that large SRS levels should not be observed at $\sim 2 \times 10^{15}$ W/cm^2, where rapid SRS growth is observed in the experiment.

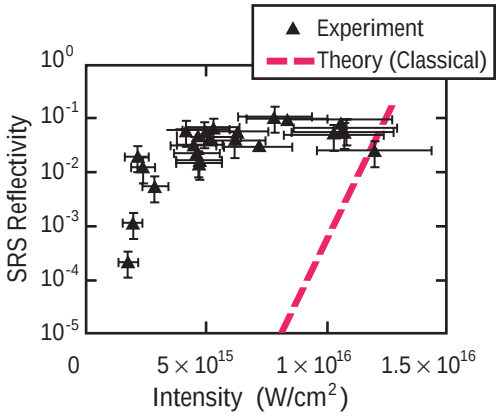

Figure8. SRS reflectivity versus peak laser intensity. The experimental data (triangles) show that the SRS instability strongly turns on at an intensity of ~ 2 $\times 10^{15}$ W/cm^2 and quickly saturates at the several percent level for higher intensities. Classical SRS theory (dashed line) fails to predict the observed SRS onset at low intensities. These data serve to guide future theoretical research for SRS.

Because other processes such as self-focusing and beam-steering physics may also be present in the experiment, a better comparison is to incorporate the classical SRS theory in the 3-D hydrodynamic code used to model the beam-steering experiments and calculate the SRS reflectivity with these other dynamic processes included. The self-focusing and beam-steering processes might change the laser conditions in the plasma compared to the vacuum laser conditions and increase the level of SRS. This type of approach is believed to be valid and has been used in the past to estimate SRS reflectivity.[8]

The modeling was performed using the measured laser and plasma initial conditions and assumed a peak intensity of 2×10^{15} W/cm^2. The model indicated that self-focusing and beam-steering physics were negligible for these laser and plasma conditions so that the laser intensity and speckle length assumed in the analytic estimate were correct. The calculated transmitted beam distribution was quantitatively similar to the measured transmitted beam and showed little beam-steering effects, which indicates that the code is correctly modeling the self-focusing and beam-steering physics. However, the 3-D model predicts negligible SRS levels at this laser intensity comparable to the simple estimates obtained from analytic theory. Because the laser intensity and speckle length are not modified by self-focusing or beam-steering physics, one can infer that the damping rate is much lower than that obtained by classical theory.

Previous large-scale experiments indicated large levels of SRS for plasma conditions where SRS was expected to be strongly damped,[5,9] but these experiments could not be fully compared with 3-D models including the effects of SRS, self-focusing, and other relevant physics. The advantage of the single-hot-spot experiment is that these comparisons can be made and indicate SRS levels much larger than classical theory predicts. These results have stimulated much recent theoretical work in wave-particle (kinetic) processes which could result in EPW damping rates much lower than classical theory values.[10,11,12] Although the SRS experiments cannot be currently modeled, they are indicating areas where the classical theory is inadequate and serve to guide future theoretical research areas.

Summary and Outlook

Single-hot-spot experiments are a fundamental approach to a quantitative understanding of laser plasma instabilities and represent a paradigm shift in this research field. The experiments are performed using laser and plasma conditions that are well characterized so that the initial conditions are well known. Flow-induced beam steering is measured and compared to 3-D direct numerical simulations. Good quantitative agreement is obtained between the experimental results and the *ab initio* model and is the first quantitative comparison between a laser-plasma instability experiment and simulation. Finally, SRS experiments were performed in a regime where the instability should be strongly damped and the SRS reflectivity was found to be large. Comparison was made to simple analytic theories and 3-D models using classical SRS theory. The classical models predict SRS significantly lower than the experimental results. These results are an example where the single-hot-spot experiments serve to guide new theoretical research.

References/Further Reading

1 J. Lindl, "Development of the Indirect-Drive Approach to Inertial Confinement Fusion and the Target Physics Basis for Ignition and Gain," *Physics of Plasmas* 2, 3933–4024 (1995).

2 H. A. Rose, D. F. Dubois, "Laser Hot Spots and the Breakdown of Linear Instability Theory with Application to Stimulated Brillouin Scattering," *Physical Review Letters* 72, 2883–2886 (1994).

3 R. G. Watt, J. Cobble, D. F. Dubois, *et al*. "Dependence of Stimulated Brillouin Scattering on Focusing Optic F Number in Long Scale-Length Plasmas," *Physics of Plasmas* 3, 1091–1095 (1996).

4 D. S. Montgomery, B. B. Afeyan, J. A. Cobble, *et al.,* "Evidence of Plasma Fluctuations and Their Effect on the Growth of Stimulated Brillouin and Stimulated Raman Scattering in Laser Plasmas," *Physics of Plasmas* 5, 1973–1980 (1998).

5 J. C. Fernández, J. A. Cobble, D. S. Montgomery, *et al.,* "Observed Insensitivity of Stimulated Raman Scattering on Electron Density," *Physics of Plasmas* 7, 3743–3750 (2000).

6 N. K. Moncur, R. P. Johnson, R. G. Watt, *et al*., "Trident: A Versatile High-Power ND-Glass Laser Facility for Inertial Confinement Fusion Experiments," *Applied Optics* 34, 4274–4283 (1995).

7 D. S. Montgomery, R. P. Johnson, H. A. Rose, *et al.,* "Flow-Induced Beam Steering in a Single Laser Hot Spot," *Physical Review Letters* 84, 678–681 (2000).

8 R. L. Berger, C. H. Still, E. A. Williams, *et al*., "On the Dominant and Subdominant Behavior of Stimulated Raman and Brillouin Scattering Driven by Nonuniform Laser Beams," *Physics of Plasmas* 5, 4337–4356 (1998).

9 D. S. Montgomery, J. D. Moody, H. A. Baldis, *et al.,* "Effects of Laser Beam Smoothing on Stimulated Raman Scattering in Exploding Foil Plasmas," *Physics of Plasmas* 3, 1728–1736 (1996).

10 B. B. Afeyan, A. E. Chou, J. P. Matte, *et al.,* "Kinetic Theory of Electron-Plasma and Ion-Acoustic Waves in Nonuniformly Heated Laser Plasmas," *Physical Review Letters* 80, 2322–2325 (1998).

11 H. X. Vu, D. F. Dubois, B. Bezzerides ,"Transient Enhancement and Detuning of Laser-Driven Parametric Instabilities by Particle Trapping," *Physical Review Letters* 86, 4306–4309 (2001).

12 H. A. Rose, D. A. Russell, in preparation (2001).